ELSEVIER

PII: S0275-5408(98)00044-1

The influence of interactions between accommodation and convergence on the lag of accommodation

Clifton Schor

Vision Science Group, School of Optometry, University of California at Berkeley, Berkeley, CA 94720-2020, USA

Summary

Several models of myopia predict that growth of axial length is stimulated by blur. Accommodative lag has been suggested as an important source of blur in the development of myopia and this study has modeled how cross-link interactions between accommodation and convergence might interact with uncorrected distance heterophoria and refractive error to influence accommodative lag.

Accommodative lag was simulated with two models of interactions between accommodation and convergence (one with and one without adaptable tonic elements). Simulations of both models indicate that both uncorrected hyperopia and esophoria increase the lag of accommodative and uncorrected myopia and exophoria decrease the lag or introduce a lead of accommodation in response to the near (40 cm) stimulus. These effects were increased when gain of either cross-link, accommodative convergence (AC/A) or convergence accommodation (CA/C), was increased within a moderate range of values while the other was fixed at a normal value (clamped condition). These effects were exaggerated when both the AC/A and CA/C ratios were increased (covaried condition) and affects of cross-link gain were negated when an increase of one cross-link (e.g. AC/A) was accompanied by a reduction of the other cross-link (e.g. CA/C) (reciprocal condition). The inclusion of tonic adaptation in the model reduced steady state errors of accommodation for all conditions except when the AC/A ratio was very high (2 MA/D).

Combinations of cross-link interactions between accommodation and convergence that resemble either clamped or reciprocal patterns occur naturally in clinical populations. Simulations suggest that these two patterns of abnormal cross-link interactions could affect the progression of myopia differently. Adaptable tonic accommodation and tonic vergence could potentially reduce the progression of myopia by reducing the lag of accommodation. ⓒ 1999 The College of Optometrists. Published by Elsevier Science Ltd. All rights reserved

Introduction

Ocular accommodation adjusts the refractive power of the eye to bring the conjugate focus of the retina into coincidence with a selected target that lies proximal to the far point of the eye. Focusing errors that result from insufficient accommodation (lags) place the conjugate focus beyond the intended target, and errors that result from excessive accommodation (leads) place the conjugate focus proximal to the target. Several static and dynamic models of accommodation which uti-

lize leaky integrators or proportional controllers represent the lag or lead of accommodation as a steady state error or byproduct of control mechanisms for accommodation (Schor, 1980; Schor and Kotulak, 1986a; Hung and Semmlow, 1980; Hung, 1991; Polak and Jones 1990; Jiang, 1996a).

Controllers refer to neurological mechanisms that transform physical stimuli such as blur and disparity to neurological codes for innervating accommodation and convergence. A leaky integrator controller is a neurological storage mechanism that builds up an innervation in response to a stimulus and it also dissipates its response when the stimulus is removed. The

decay requires that a small error remain to keep the stored response from decaying. A physiological analog to this is a population of tonic cells that would gradually increase firing rate when stimulated and would store the response for a limited time when the stimulus was removed. The rate at which the response decays when the stimulus is removed defines the time constant of the integrator. Stimuli are blur and disparity of the retinal image that are reduced as the control system responds. A proportional controller is a neurological mechanism that provides an innervation that is proportional to the magnitude of the error signal (i.e. retinal image blur). A physiological analog to this is a population of phasic cells that would abruptly increase their firing rate to a magnitude that is proportional to the amplitude of the error signal and would rapidly decay when the error signal was removed. As with the leaky integrator controller, an error signal is needed to maintain a constant response and prevent the rapid decay which occurs in the absence of a stimulus. Although these two types of controllers differ mathematically, they make similar predictions for the error signal needed to maintain a steady response (steady state error). The lag of accommodation is an example of a steady state error. It is a constant difference in the response and a fixed stimulus distance. A first order plant mechanism refers to a description of the dynamics of the lens, ciliary body and extra ocular muscle responses with a position and velocity term. The nonlinear compression limit to be described later is a mathematical tool that is needed to keep the simulations of motor responses stable or within bounds. The stimulus to the tonic integrator needs to remain small, otherwise the response becomes infinitely large. A physiological analog to this would be a limited number of tonic cells with very long time constants, whose response became saturated when the stimulus was too large. Response gain refers to the ratio of the response over the stimulus. AC/A and CA/C ratios are examples of the gain of accommodative vergence and vergence accommodation.

The magnitude of these steady state errors is inversely related to the gain and decay time constants of the controllers. Other factors influence the steady state error of accommodation by increasing or decreasing the demands on the accommodative controller. These factors include optical and motor biases such as refractive errors and resting focus, and tonic after effects of accommodation Schor 1979a; Schor and Kotulak, 1986b). Demands on accommodation are also influenced by synergistic cross-link interactions between accommodation and vergence in which optically stimulated accommodation evokes convergence (accommodative convergence) (Alpern and Ellen, 1956) and disparity stimulated vergence evokes accom-

modation (convergence accommodation) (Fincham and Walton, 1957). The magnitude of these cross-link interactions is quantified as a gain function where meter angles of convergence associated with one diopter of accommodation is termed the AC/A ratio (MA/D) and diopters of accommodation stimulated by a meter angle of convergence is termed the CA/C ratio (D/MA). A meter angle describes vergence magnitude as the reciprocal of the viewing distance in meters. Meter angles are converted to units of prism diopters by multiplying them by the interpupillary distance in centimeters. Thus a target at 50 cm subtends a 2 MA stimulus to convergence which is equivalent to 12 prism diopters for a person with a 6 cm interpupillary distance. These gains are quantified (e.g. AC/A) when the negative feedback loop of the stimulated system (e.g. accommodation) is closed while the feedback loop of the associated system (e.g. convergence) is open (e.g. by occluding one eye). In the case of the CA/C ratio, the feedback loop of the accommodative system can be opened using pin hole pupils or a low spatial frequency stimulus while the feedback loop for convergence is closed (binocular viewing conditions) (Tsuetaki and Schor, 1987).

Under normal binocular viewing conditions, both the accommodation and convergence feedback loops are closed, allowing biases of both systems to influence the accuracy of accommodation in several ways. Accommodation bias and refractive error are subtracted from the error signal for accommodation via a negative feedback loop. This difference influences the magnitude of the accommodative stimulus which determines the steady state error of the accommodative controller. Accommodative bias and refractive error also influence accommodative vergence which feeds back with the other vergence components to influence convergence accommodation and affect the accuracy of accommodation. Vergence phoria (bias) and adaptable tonic convergence feedback to the error signal for vergence and the phasic controller response to the resulting vergence error stimulates the convergence accommodation link to influence steady state errors of accommodation.

Prediction of steady state errors of accommodation is facilitated with computer simulations using models of these complex mutual interactions between accommodation and vergence control. The current paper examines the influence of interactions between cross-links with biases of the convergence and accommodative systems to illustrate combinations of parameters that lead to the large and small steady state errors of accommodation while both systems operate under closed-loop conditions. These predictions may be useful in identifying combinations of clinical risk factors or syndrome precursors to myopia in situations where

retinal image blur produced by steady state errors of accommodation guide the emmetropization process (Gwiazda *et al.*, 1993; Jiang, 1995; Wallman and McFadden, 1995; Goss and Zhai, 1994; Abbott, *et al.*, 1998).

Models of cross-link interactions

There are several heuristic models of cross-link interactions between accommodation and convergence and each emphasizes a particular aspect of the synergistic reflexes (e.g. biases and static behavior (Hung and Semmlow, 1980; Jiang, 1996a), dynamic responses and tonic adaptation (Schor and Kotulak, 1986a; Hoffmann and Bielchowsky, 1900; Schor, 1979b; 1992; Ebenholtz and Fisher, 1982; Wick and London, 1987; Rosenfield and Gilmartin, 1988; Lakkis and Bruce, 1989; Hung, 1992; Jiang, 1996b). All of these models of adaptation use a leaky integrator controller with a long decay time constant. In one model, the time constant is modified during adaptation (Hung, 1991), whereas the other models have two leaky integrators, one phasic (fast) and one tonic (slow) that have short and long time constants respectively. The total accommodative response equals the sum of activity of the phasic and tonic controllers. Steady state errors or lags of accommodation are greater with the phasic elements than the tonic, because the phasic elements have shorter decay time constants and lower steady state gains. Accordingly the lag of accommodation decreases as more of the total accommodative response is controlled by the tonic element. After effects of accommodation provide an estimate of the magnitude of the tonic component of the accommodative response. In all of these models, the after effects of accommodation and vergence are determined by the gain and time constant of the tonic element at the time the after effect is measured following the adaptation stimulus.

The model used in the current investigation represents adaptive behavior resulting from tonic accommodation and tonic convergence and its impact on cross-link interactions. This model was selected because it embodies both the static and dynamic behavioral characteristics of interactions between accommodation and convergence (Schor, 1992). Several behaviors are uniquely predicted by this model. Tonic accommodation and tonic convergence, respectively, have been shown not to stimulate accommodative vergence and vergence accommodation under the open-loop conditions in which these cross-link gains are normally measured (Schor and Kotulak, 1986a,b; Jiang 1996a,b). Accommodative vergence causes vergence after effects and vergence accommodation produces accommodative after effects (Schor and Kotulak, 1986a) and the relative gains of tonic accommodation

and tonic convergence influence the magnitude of the AC/A and CA/C ratios (Schor and Tsuetaki, 1987; Schor, 1988; Schor and Horner, 1989). In this paper, the effects of tonic controllers on steady state errors of accommodation are illustrated by comparing simulations of the adaptation model (*Figure 1(a)*) to another model that lacks tonic elements (Schor and Narayan, 1982) (*Figure 1(b)*).

As is illustrated in *Figure 1*, both models contain cross-links with adjustable gains and biases in the form of the distance vergence phoria and refractive error. Accommodative bias could also include a motor component described as the resting focus (Hung and Semmlow, 1980), but to simplify the model, all the accommodative biases have been consolidated into a single value described in terms of refractive error. This consolidation does not assume that the resting focus is zero. Normally the resting focus of accommodation is at some finite viewing distance (1.5D) (Schor *et al.*, 1984). In the current simulations, the values of true optical measures of refractive error would be reduced for myopia and increased for hyperopia by the resting focus of accommodation.

To investigate the influence of accommodation and vergence biases on cross-link interactions, a bias estimate of accommodation has been made with vergence clamped at zero (binocular viewing through pinholes at an infinite viewing distance) and the vergence bias estimate is made from the distance phoria with accommodation clamped at zero (monocular viewing at an infinite viewing distance). These measures of resting levels of accommodation and vergence are made with the measured loop and the cross-coupled loop closed (e.g. vergence open and accommodation closed for vergence bias). Resting accommodation and vergence can also be measured with both loops opened, such as dark focus and dark vergence. However for several reasons, these are inappropriate measures of bias to investigate cross-link interactions. In darkness, these dark measures of bias are influenced by an idiosyncratic sense of proximity (Schor and McLin, 1988) and both vergence and accommodation are free to change allowing them to influence one another in darkness (Kotulak and Schor, 1986b).

The vergence and accommodation biases are located at the outputs of their respective systems so that their magnitudes will represent values that correspond to the behavioral measures in units of meter angles (MA) and diopters (D) respectively. Both models contain an error detector which has a threshold or dead zone, a pure delay to represent the latency, a phasic controller represented as a first order lag element, independent gain adjustments of the two cross-links, and a first order plant mechanism. Both models also have a non-linear range limit at the output to represent the natural
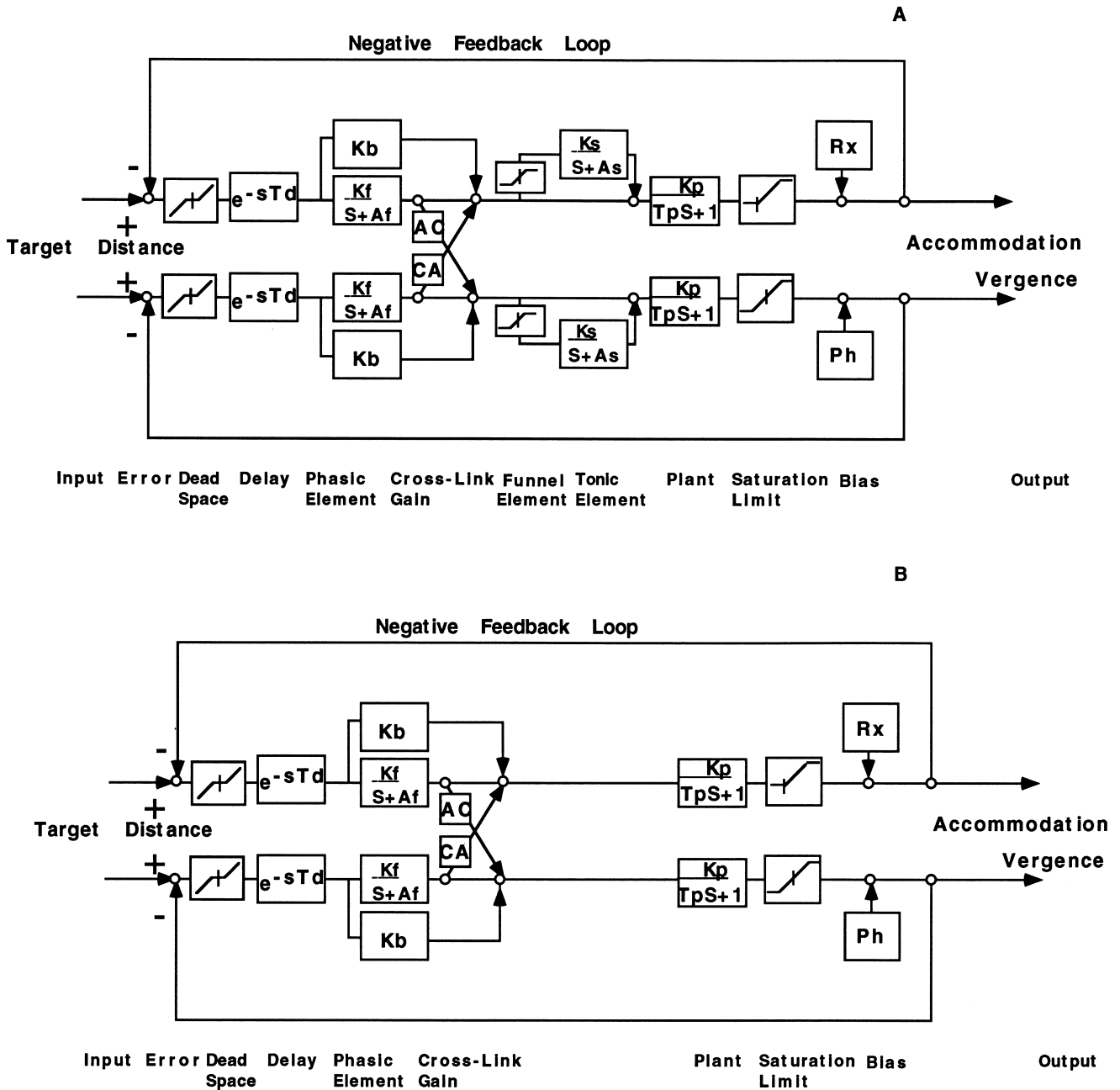
A

B

Figure 1. Block systems diagram of the phasic-tonic control (a) and phasic control (b) of and interactions between accommodation and vergence. The tonic integrator in (a) is preceded by a compression (funnel) input limiter and the system output is limited by a natural range limit. The dead zone represents the threshold error or stimulus, and the pure delay represents the latency. Biases (refractive error and far heterophoria) are placed at the end of the feed-forward loop so that their magnitude and units are represented by clinical measures. The organization of these blocks is taken from the model of disparity vergence proposed by Schor and Kotulak (1986a).

boundaries or operating ranges of accommodation and vergence. These boundaries correspond to the monocular amplitude of accommodation and the convergence (base-out) to divergence (base-in) amplitudes of disparity vergence (Hofstetter, 1983). The dead zone for accommodation (depth of focus) and vergence are not included in the simulations since they were not varied

and are very small (Riggs and Neihle, 1960; Green *et al.*, 1980; Kotulak and Schor, 1986a) such that they have negligible impact on the lag of accommodation. An additional non-linearity of the adaptable model limits the magnitude of the input to tonic controllers with a compression or funnel limiter that allows sustained tonic responses to small inputs while it prevents

Table 1. Values of fixed model parameters including gains and time constants for the phasic and adaptable controllers and plants, and the non-linear operators

Fixed model parameters	Vergence	Accommodation
Gains: (steady state gain = K* time constant)		
Kb (proportional)	1.5	1.5
Kf (phasic)	2.5	2.5
Ks (tonic)	1.5	1.5
Kp plant	0.3	0.25
Time constants: (T = 1/a)		
T (proportional)	1.0	1.0
Tf (phasic)	5 s	5 s
Ts (tonic)	20 s	20 s
Tp (plant)	0.15 s	0.25 s
Td (delay)	0.15 s	0.30 s
Non-linearities:		
Compression limit	0.35 MA	0.35 D
Range limit	−2.5 to +5 MA	0–15 D

excessively large tonic responses to large inputs (Schor, 1992; Hung, 1992). It also limits the maximum rate and amplitude of tonic responses and provides stability to dynamic responses (Schor, 1992).

Simulations

Accommodative lag was simulated with both models of interactions between accommodation and convergence (one with and one without tonic elements). Simulations were of steady state errors of accommodative as a function of bias (either refractive error or heterophoria) and cross-link gain (variations of either AC/A, CA/C or both). Steady state errors of accommodation were computed with a digital computer simulator (TUTSIM℗ from Applied i) in response to a near step stimulus (60 s duration) representing a change from infinity to a 40 cm viewing distance (2.5 D and 2.5 MA). *Table 1* lists the values of fixed model parameters, including gains and time constants for the phasic and tonic controllers and plants, and the non-linear operators described above. These are the same values used previously to demonstrate the dynamic and static performance of the model (Schor, 1992). In that paper, these values were shown to yield frequency responses and stability similar to empirical measures of dynamic vergence and accommodation. *Table 2* lists model parameters that were varied to include the two cross-link gains (AC/A and CA/C) and biases (vergence phoria and refractive error). In prior versions of this model (Schor and Kotulak, 1986a) the cross-link gain (AC) was set at 1.0 to emphasize how dramatically the balance of tonic elements for accommodation and vergence could vary the behavioral measures of AC/A. However it is likely that additional factors influence the whole system cross-link interactions. Accordingly, adjustable cross link gains (AC and CA) were added to represent these other factors with a

Table 2. Values of varied model parameters including bias (refractive errors and far heterophoria), system cross-link gains, and internal model values of CA and AC that produced these gains

Varied model parameters		Vergence			Accommodation	
Bias		+2 MA			+2 D	
Cross-link gains		0.188 to 1.5 D/MA			0.33 to 2 MA/D	
AC/A (MA/D)	AC non adapt	AC adapt	CA/C (D/MA)	CA non-adapt	CA adapt
---	---	---	---	---	---
2	1.7	1.88	1.5	1.8	2.0
1.66	1.41	1.56	1.25	1.5	1.66
1.33	1.13	1.25	1	1.2	1.33
1.0	0.85	0.94	0.75	0.9	1.0
0.66	0.56	0.62	0.375	0.45	0.5
0.33	0.28	0.31	0.188	0.225	0.25

single variable and also to allow variation of the behavioral AC/A and CA/C ratios, independently of the gain and time constants of the tonic elements.

Simulated values of AC/A and CA/C depend on the gains of phasic and tonic controllers plus the plant gain as well as the gain of the AC and CA cross-links. These parameters have been derived by Polak and Jones (1990). The values of AC and CA used in the simulation (*Table 2*) were selected to yield the whole system measures of AC/A and CA/C that represent the range of values normally encountered in clinical populations (Sheedy and Saladin, 1983). Thus, all of the varied parameters (independent variables) represent measurable functions that are routinely quantified in clinical examinations. These independent variables include distance heterophoria, refractive error, AC/A and CA/C ratios and the dependent variable was the lag of accommodation.

Simulations predicted the steady state errors of accommodation with a sign convention of positive for lag and negative for lead. Esophoria and myopia biases are positive and exophoria and hyperopia biases are negative. The negative dioptric vergence and crossed disparity of a near target are stimuli to increase accommodation and convergence. Simulations were conducted with either one of the cross-links fixed at a normal value while the other was varied (clamped conditions) or with both cross-links varied in the same direction (covarying condition) or in opposite directions (reciprocal condition).

The results that follow demonstrate that accommodative lag depends upon a combination of factors and the results illustrate trends or qualitative aspects resulting from interactions between bias and cross-link gains. The quantitative estimates of lag of accommodation should not be taken literally since different heuristic models will predict slightly different magnitudes for the lag; however all models will yield the same trends. None of the models described above are known to be homeomorphic with the physiological structure and functional organization of the accommodative-vergence system (Judge and Cumming, 1986; Mays and Gamlin, 1995). The control models have been constructed to approximate or predict behavior based upon static and dynamic behavioral measures. The constants used in the various models, such as those shown in *Table 1*, will vary between models because their mathematical structures differ and also because models have been designed to predict different types of behavior such as static and dynamic. If the models are accurate, then they will make similar predictions about the lag of accommodation, even though their structure is different.

Results

General observations: all graphs plot the lag of accommodation on the Y axis as a function of two independent variables. These are the gains of cross-link interactions on the X axis (AC/A, CA/C or their combination) and bias on the Z axis (refractive error or distance heterophoria). Note that in the data plots, the signs of hyperopia and myopia were made positive and negative respectively to enhance the perspective view of the 3-D graphs. The physical limits to the error of accommodation depend upon the dioptric target vergence, refractive error and amplitude of accommodation. The maximum possible lag equals the hyperopic refractive error plus the dioptric vergence of the target. In these simulations the maximum hyperopic bias was 2D so the largest lag possible was 4.5D. The maximum possible lead equals the sum of the amplitude of accommodation and maximum diopters of myopia, minus the dioptric vergence of the target. In these simulations the amplitude of accommodation was 15D so the largest lead possible was 14.5D. In the heterophoria simulations, the lag of accommodation never exceeds 2.5 diopters because the refractive state was fixed at zero (emmetropia). The difference graphs (c) represent the change in lag predicted by the adaptable minus the non-adaptable model simulations. Negative values indicate conditions in which the lag was reduced by tonic adaptation or when the lead of accommodation was increased by tonic adaptation. Positive values indicate conditions in which the lead was reduced by tonic adaptation or when the lag of accommodation was increased by tonic adaptation. Increases and decreases occur when values plotted in the difference curve (c) have the same or opposite sign respectively as the predictions of the adaptation model (a).

Clamped CA/C condition: the CA/C was clamped at a value of 0.75 D/MA which represents a normal gain for a young adult (Fincham, 1955). AC/A ratios were varied from 0.33 to 2.0 MA/D in steps of 0.33, where the normal gain is 0.66 MA/D which corresponds to 4Δ/D (Flom, 1960; Ogle, 1966). Accommodative lag was computed for each of these AC/A ratios as a function of far heterophoria (ranging from 2 MA exophoria to 2 MA esophoria in steps of 0.5 MA). The results for the adaptable phasic-tonic model, the non-adaptable phasic model and their difference (adaptable–non-adaptable) are shown in *Figure 2 (a),(b)*, and *(c)* respectively. *Figure 2(a), (b)* illustrates that the steady state error of accommodation increased monotonically with heterophoria bias and the steady state errors increased as the AC/A ratio increased. Comparison of the simulations of the adaptive and non-adaptive models illustrates that adaptation
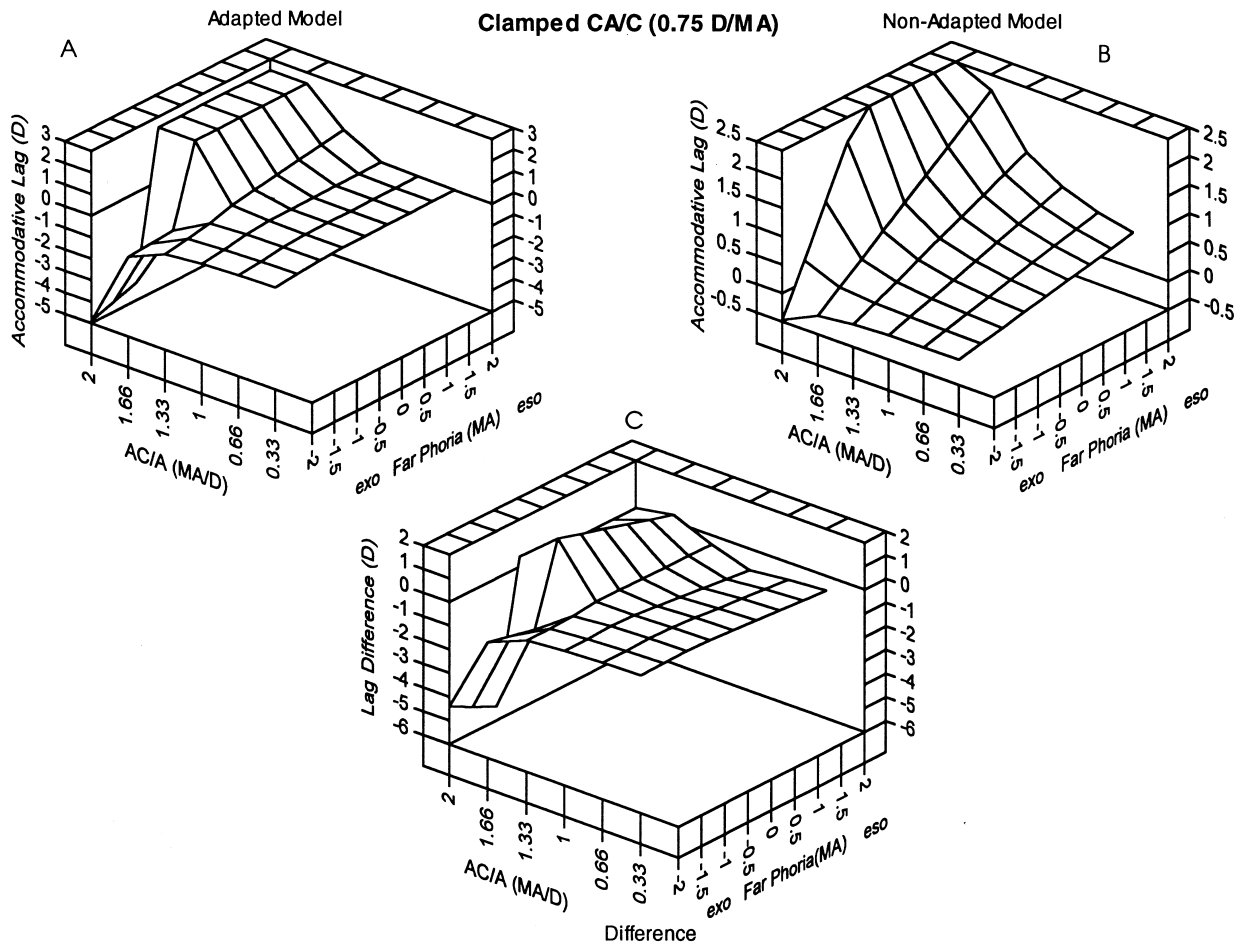
Figure 2. Simulations of accommodative lag as a function of distance heterophoria for the clamped CA/C condition are shown for the adaptable and non-adaptable models and their difference in (a), (b), and (c) respectively. (a) and (b) illustrate monotonic increases of the steady state error of accommodation plotted as a function of heterophoria bias and the AC/A ratio. (c) plots the difference between predictions of the adaptable (a) and the non-adaptable (b) model and illustrates that adaptation reduced the steady state errors of accommodation when the AC/A ratio was less than 1.66 MA/D (10D/D).

reduced the steady state errors of accommodation when the AC/A ratio was less than 1.66 MA/D ($10\Delta/$D). When the AC/A ratio was high the accommodative response lagged behind the stimulus for ortho and small distance exophorias because of the near esophoria stimulated by the high AC/A ratio. The difference graph shown in *Figure 2(c)* reveals that the lag was reduced by tonic adaptation (the difference is negative and has the opposite sign as in *Figure 2(a)* for AC/A values less than 1.66 MA/D, and the lag and lead were increased by tonic adaptation (the difference assumes large positive and negative values that have the same sign as in *Figure 2(a)*) for the two largest values of the AC/A. Steady state errors of accommodation for higher AC/A ratios are very large for the adaptable model and they resulted in the discontinuity of the function along the Z axis.

Simulations of accommodative lag as a function of refractive error for the clamped CA/C condition are shown for the two models and their difference in *Figure 3 (a),(b)*, and *(c)* respectively. The same trends are present as in *Figure 2*. The leads and lags of accommodation associated with myopia and hyperopia respectively are smaller for the adaptation model when the AC/A ratio was less than 1.66 MA/D (*Figure 3 (c)*). As with the phoria variation, steady state errors of accommodation were very large for higher AC/A ratios in the adaptable model (*Figure 3(a)*) compared to the non-adaptable model (*Figure 3(b)*). When the AC/A ratio was high the accommodative response lagged behind the stimulus for emmetropes and small degrees of myopia because of the near esophoria stimulated by the high AC/A ratio. Refractive variations produced greater steady state errors of accom-
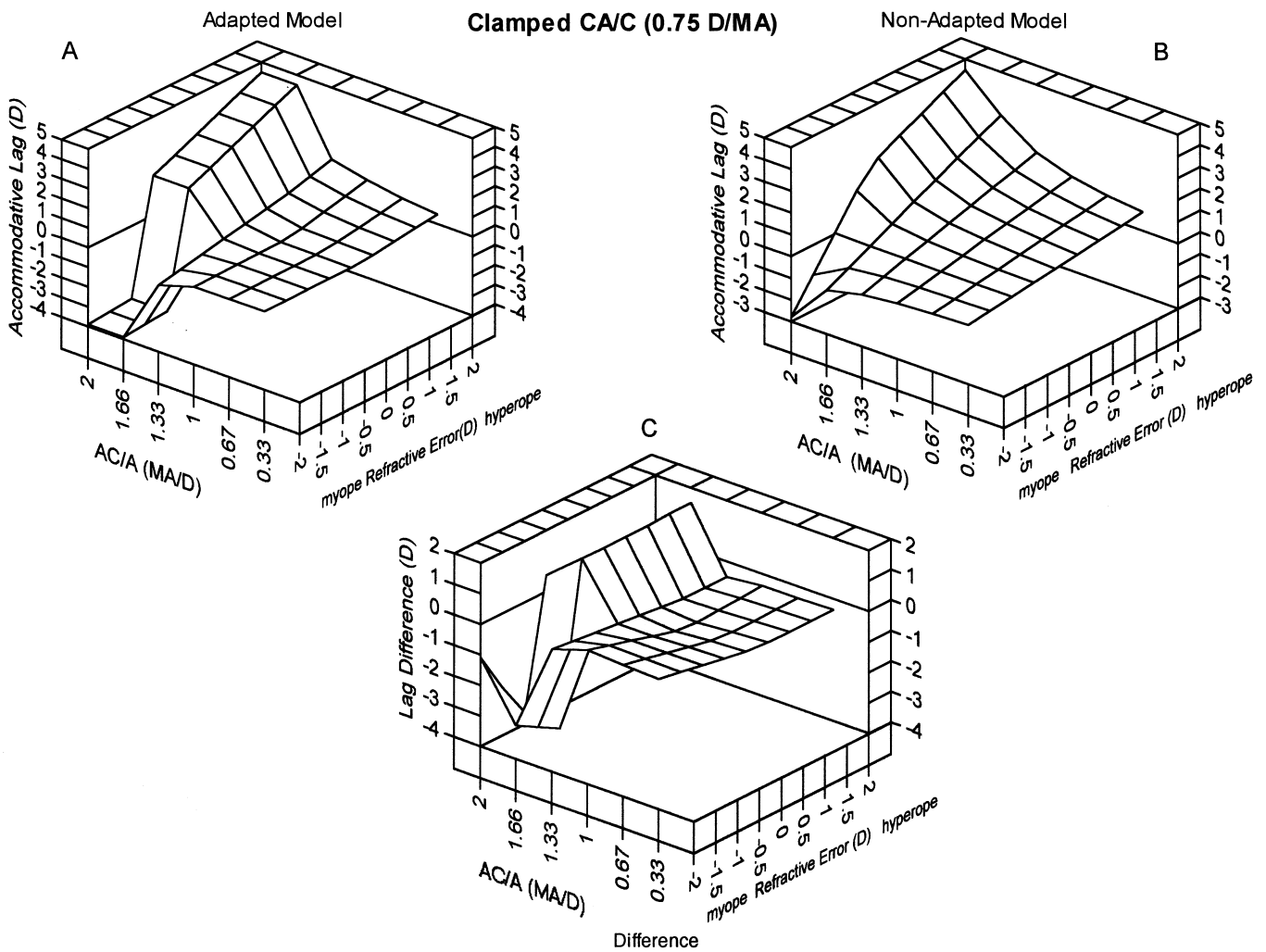
Figure 3. Simulations of accommodative lag as a function of refractive error for the clamped CA/C condition are shown for the adaptable and non-adaptable models and their difference in (a), (b), and (c) respectively. (a) and (b) illustrate monotonic increases of the steady state error of accommodation plotted as a function of refractive error bias and the AC/A ratio. (c) plots the difference between predictions of the adaptable (a) and the non-adaptable (b) model and illustrates that adaptation reduced the steady state errors of accommodation when the AC/A ratio was less than 1.66 MA/D (10D/D).

modation over the whole range of AC/A ratios for both the adaptive and non-adaptable models (*Figure 3(a),(b)*) than did phoria variations (*Figure 2(a),(b)*).

Clamped AC/A condition: the AC/A was clamped at a value of 0.66 MA/D which corresponds to the normal gain of the response AC/A ratio (4Δ/1D) (Flom, 1960; Ogle, 1966). CA/C ratios were varied from 0.375 to 1.5 D/MA in steps of either 0.375 or 0.25 D/MA. Accommodative lag was computed for these CA/C ratios as a function of the same range of far heterophorias used in the clamped CA/C condition. The results for the adaptable phasic-tonic model, the non-adaptable phasic model and their difference (adaptable–non-adaptable) are shown in

Figure 4(a),(b) and *(c)*, respectively. *Figure 4(a),(b)* illustrates that the steady state error of accommodation increased monotonically with heterophoria bias and the steady state errors increased as the CA/C ratio increased. When the CA/C ratio was high the accommodative response lead the stimulus for orthophoria because of the excessive convergence accommodation stimulated by the high CA/C ratio. Comparison of the simulations of the adaptive and non-adaptive models illustrates that tonic adaptation reduced the steady state errors of accommodation for all values of the CA/C (values of the difference curve in *Figure 4(c)* are of opposite sign to those predicted by the adaptation model in *Figure 4(a)*).
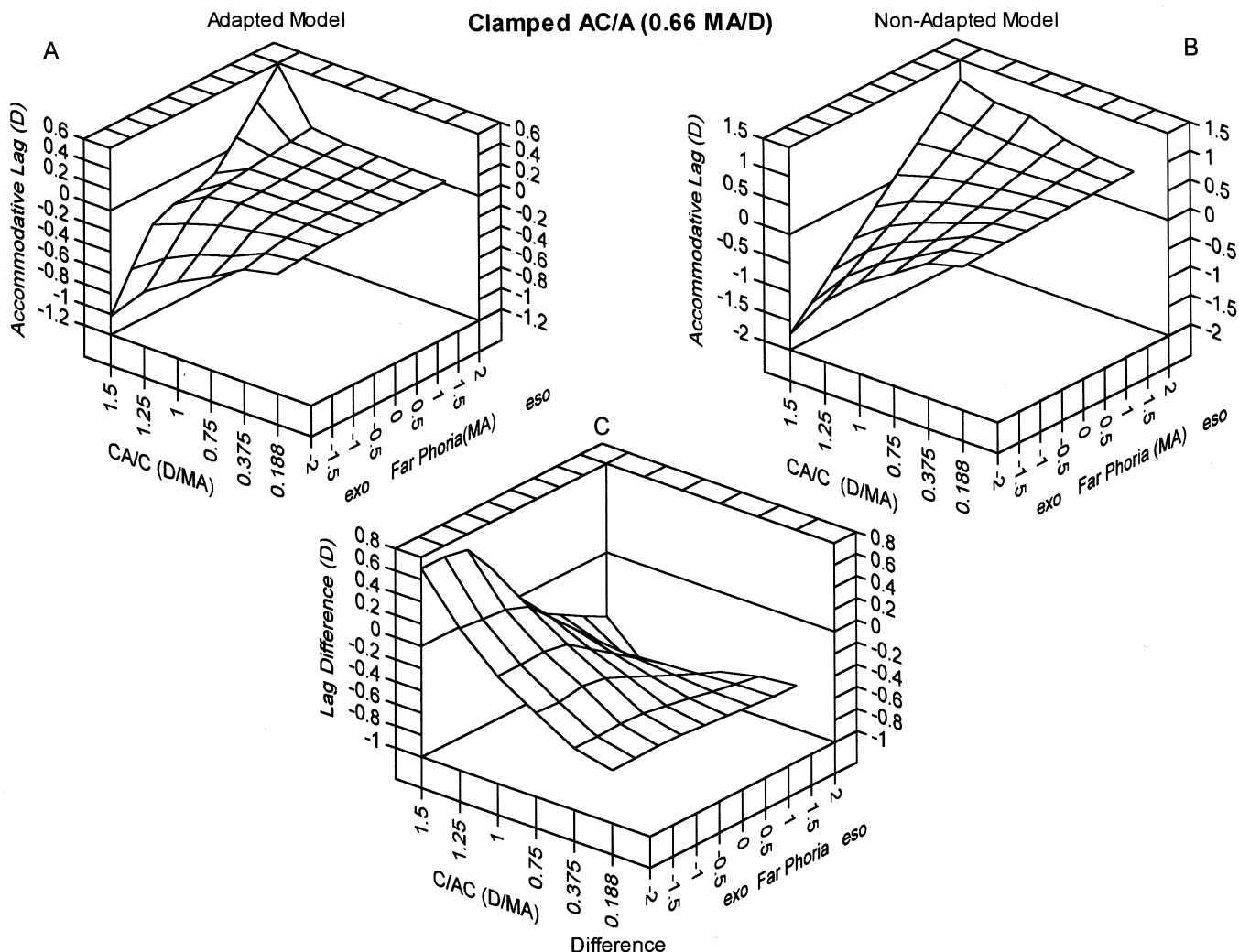
Figure 4. Simulations of accommodative lag as a function of distance heterophoria for the clamped AC/A condition are shown for the adaptable and non-adaptable models and their difference in (a), (b), and (c) respectively. (a) and (b) illustrate monotonic increases of the steady state error of accommodation plotted as a function of far heterophoria bias and CA/C ratio. (c) plots the difference between predictions of the adaptable (a) and the non-adaptable (b) model and illustrates that adaptation reduced the steady state errors of accommodation for all values of the CA/C ratio.

Simulations of accommodative lag as a function of refractive error for the clamped AC/A condition are shown for the two models and their difference in *Figure 5(a),(b)*, and *(c)*, respectively. The same trends are present as shown in *Figure 4*. The leads and lags of accommodation associated with myopia and hyperopia respectively are smaller for the adaptation model for CA/C ratios less than 1.5 D/MA and they are slightly larger for combinations of the highest CA/C ratio with hyperopic refractive errors (*Figure 5(c)*). When the CA/C ratio was high the accommodative response led the stimulus for emmetropia because of the excessive convergence accommodation stimulated by the high CA/C ratio. The steady state errors of accom-

modation produced by the non-adaptive model were approximately the same for variations of heterophoria (*Figure 4(b)*) and refraction (*Figure 5(b)*); however steady state errors of accommodation produced by the adaptive model were smaller for variations of heterophoria (*Figure 4(a)*) than for refractive error (*Figure 5(a)*).

Covarying condition: the AC/A and CA/C gains were increased together from low values of 0.188 D/MA and 0.33 MA/D to higher values of 1.0 D/MA and 1.33 MA/D. Because the covaried condition led to extremely large steady state errors of accommodation when the ratios exceeded this range, accommodative lag is only shown for the four covarying values indi-
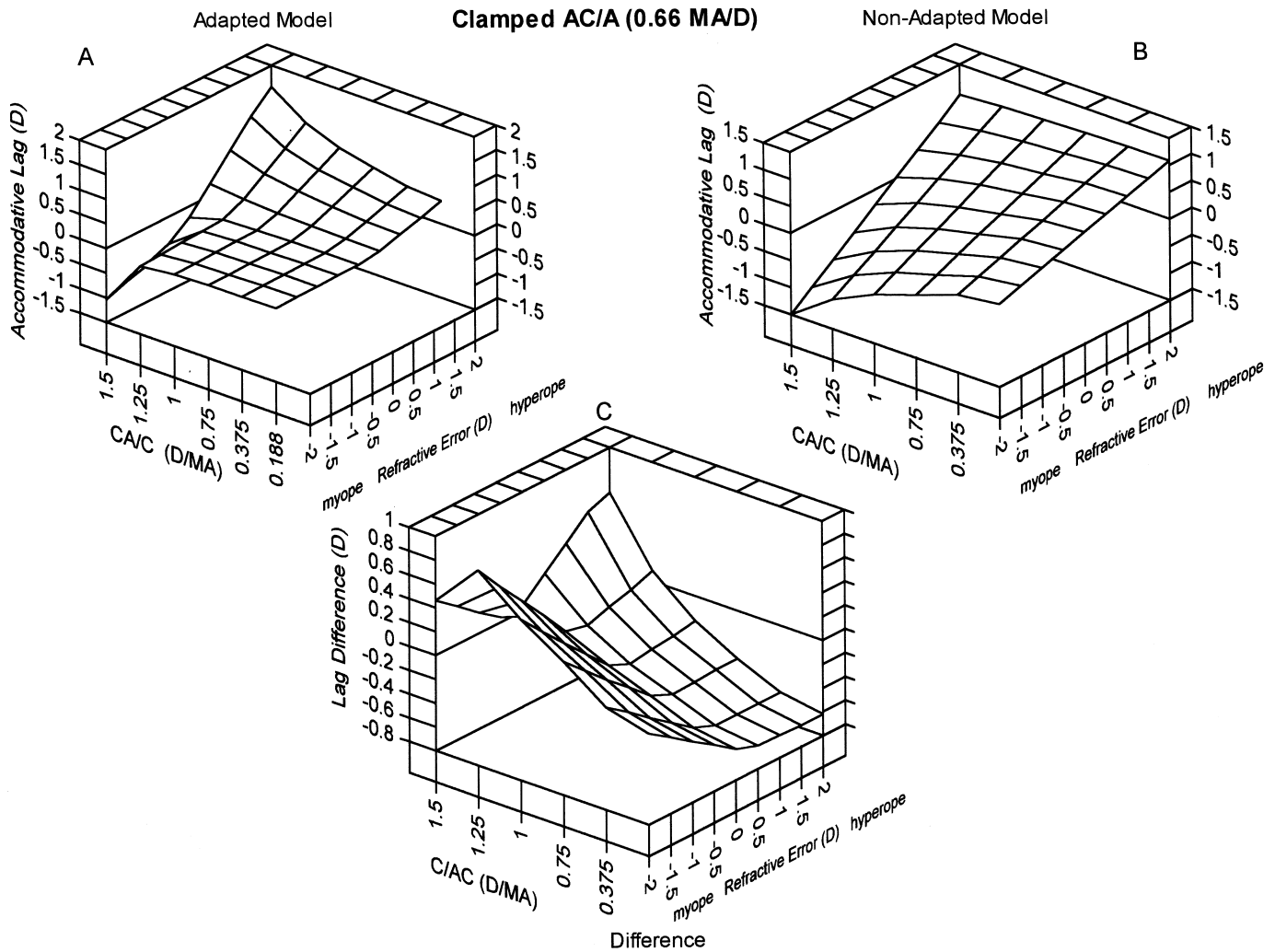
Figure 5. Simulations of accommodative lag as a function of refractive error for the clamped AC/A condition are shown for the adaptable and non-adaptable models and their difference in (a), (b), and (c) respectively. (a) and (b) illustrate monotonic increases of the steady state error of accommodation plotted as a function of refractive error and CA/C ratio. (c) plots the difference between predictions of the adaptable (a) and the non-adaptable (b) model and illustrates that adaptation reduced the steady state errors of accommodation when the CA/C ratio was less than 1.5 D/MA. The lag of accommodation was increased by adaptation for combinations of the highest CA/C ratio and hyperopic refractive errors.

cated along the X axis of the plots. Accommodative lag was computed for these four combinations as a function of the same range of far heterophorias used in the prior two conditions. The results for the adaptable phasic-tonic model, the non-adaptable phasic model and their difference (adaptable–non-adaptable) are shown in *Figure 6(a),(b)* and *(c)* respectively. *Figure 6(a),(b)* illustrates that the steady state error of accommodation increased very rapidly with heterophoria bias and the steady state errors increased with combined elevation of the AC/A and CA/C ratios. Comparison of the simulations of the adaptive and non-adaptive models illustrates that tonic adaptation reduced the steady state errors of accommodation

when the covarying AC/A and CA/C ratios were less than 1.00 MA/D and 1.33 D/MA respectively. Over this range of cross-link gains, the difference graph shown in *Figure 6(c)* is negative and opposite in sign to *Figure 6(a)*. Steady state errors of accommodation for the adaptation model (*Figure 6(a)*) and the difference curves (*Figure 6(c)*) are very large and of the same sign for the higher values of cross-links (1.33 and 1.0) and they result in the discontinuity of the function along the Z axis as the error switches from a lag to a lead at zero bias.

Simulations of accommodative lag as a function of refractive error for the covarying condition are shown for the two models and their difference in
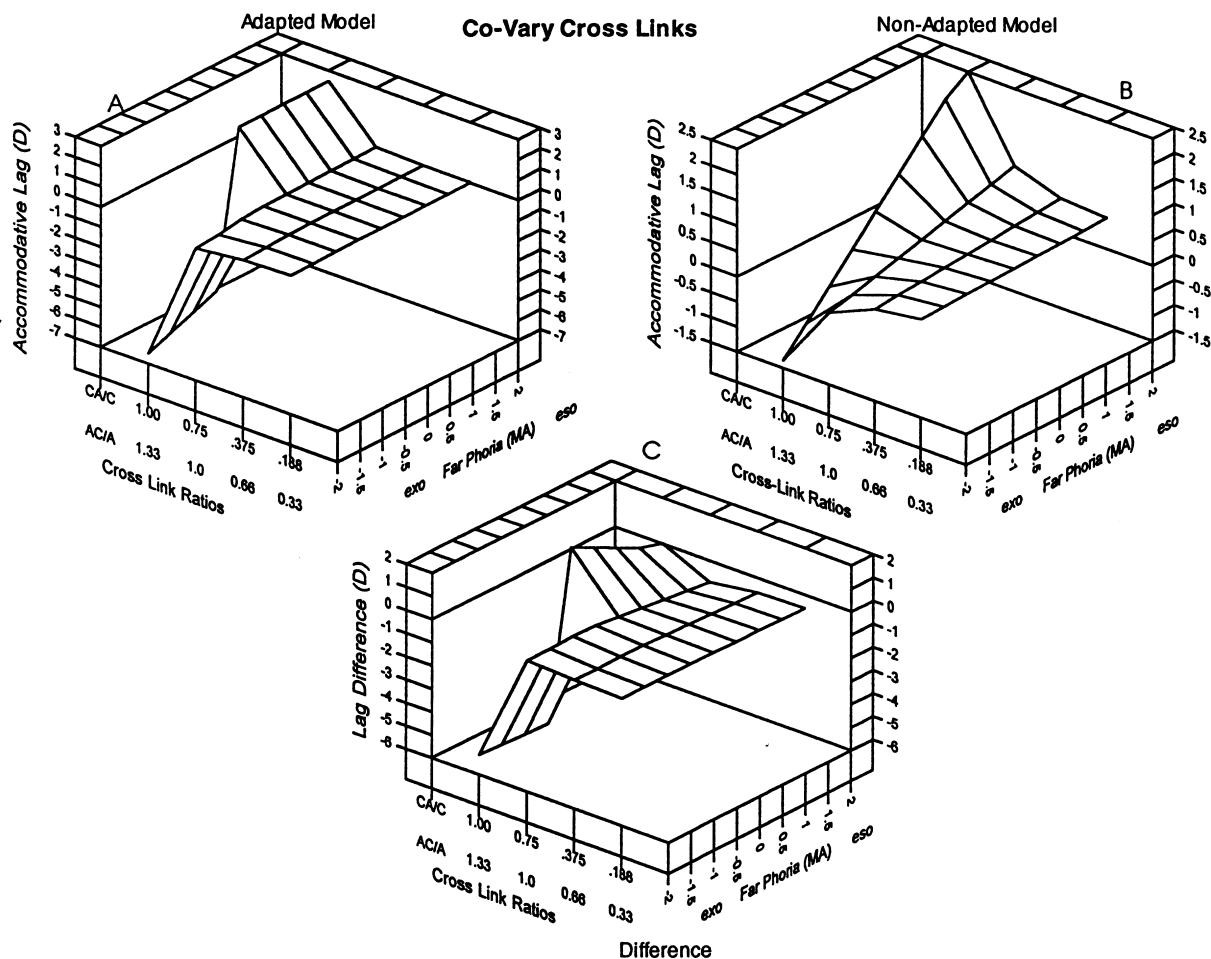
Figure 6. Simulations of accommodative lag as a function of far heterophoria for the covaried condition are shown for the adaptable and non-adaptable models and their difference in (a), (b), and (c) respectively. (a) and (b) illustrate that the steady state error of accommodation increased with far heterophoria bias and the steady state errors increased rapidly with combined elevation of the AC/A and CA/C ratios. (c) plots the difference between predictions of the adaptable (a) and the non-adaptable (b) model and illustrates that adaptation reduced the steady state errors of accommodation when the covarying AC/A and CA/C ratios were less than 1.00 MA/D and 1.33 D/MA.

Figure 7(a,b), and *(c)* respectively. The same trends are present as shown in *Figure 6*. The leads and lags of accommodation associated with myopia and hyperopia respectively are smaller for the adaptation model for covarying ratios less than 1.00 MA/D and 1.33 D/MA and larger for the higher ratios of the adaptable model (*Figure 7(c)*). The steady state errors of accommodation produced by the adaptive and non-adaptive models were approximately the same for variations of heterophoria (*Figure 7(a,b)*) and refraction (*Figure 7(a,b)*).

Reciprocal condition: the AC/A and CA/C gains were varied reciprocally such that at one extreme a low value of the CA/C (0.188 D/MA) was paired with a high value of the AC/A (1.66 MA/D), and at the opposite extreme a high value of the CA/C (1.25 D/

MA) was paired with a low value for the AC/A (0.33 MA/D). Accommodative lag was computed for the 5 pairs of cross-link gains shown on the X axis as a function of the same range of far heterophorias as used above. The results for the adaptable phasic-tonic model, the non-adaptable phasic model and their difference (adaptable–non-adaptable) are shown in *Figure 8(a),(b)* and *(c)* respectively. *Figure 8(a,b)* illustrates that heterophoria produced smaller changes in the steady state error of accommodation than found when only one cross link was varied and the other was clamped (*Figures 2–5*). The steady state errors of accommodation associated with a given heterophoria remained fairly constant for various reciprocal combinations of cross-link ratios. Comparison of the simulations of the adaptive and non-adaptive models
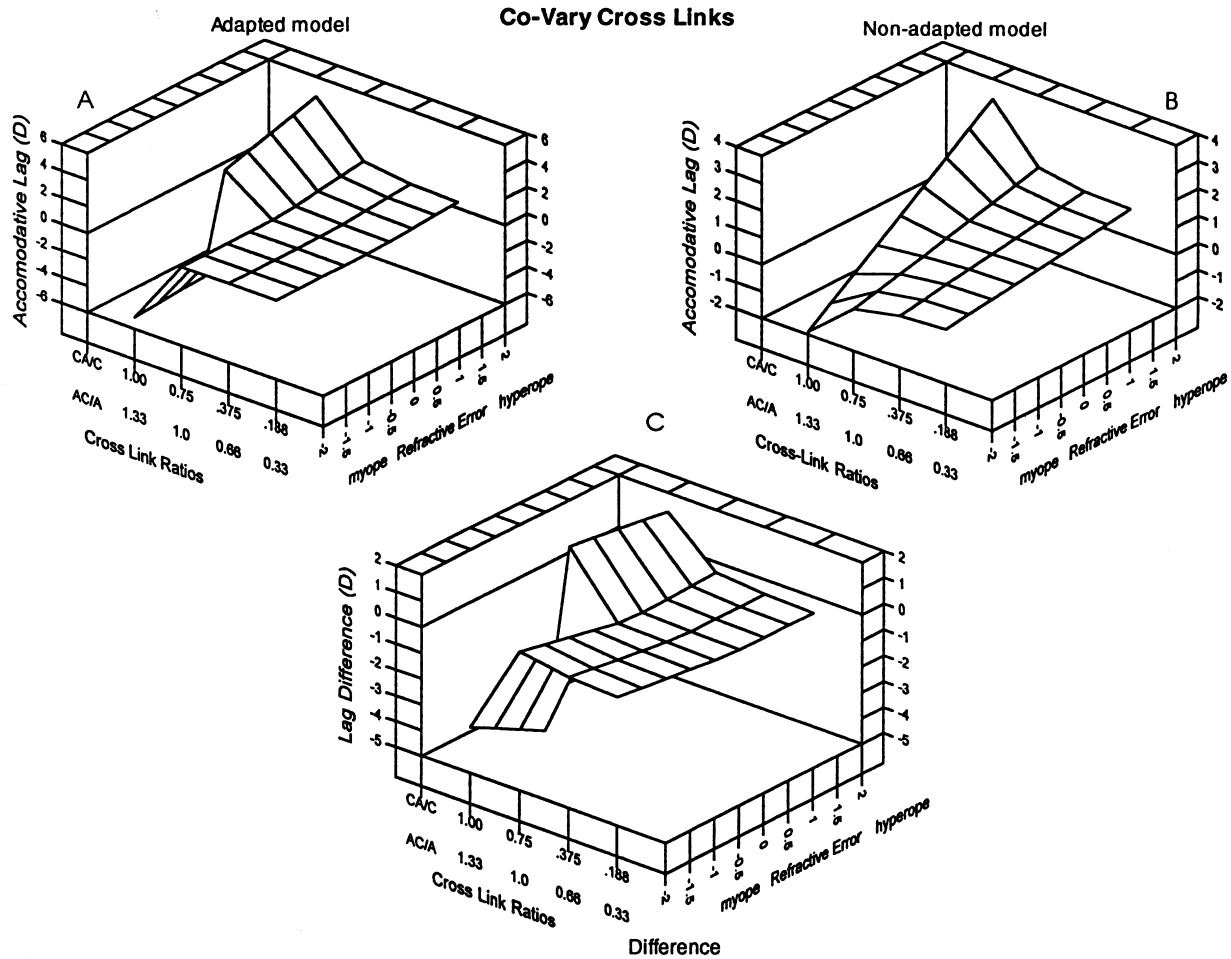
Figure 7. Simulations of accommodative lag as a function of refractive error for the covaried condition are shown for the adaptable and non-adaptable models and their difference in (a), (b), and (c) respectively. (a) and (b) illustrate that the steady state error of accommodation increased with refractive error and the steady state errors increased rapidly with combined elevation of the AC/A and CA/C ratios; (c) plots the difference between predictions of the adaptable (a) and the non-adaptable (b) model and illustrates that adaptation reduced the steady state errors of accommodation when the covarying AC/A and CA/C ratios were less than 1.00 MA/D and 1.33 D/MA.

illustrates that tonic adaptation reduced the steady state errors of accommodation over the entire range of heterophoria with the largest reductions for low values of the CA/C ratio combined with high values of the AC/A ratio (*Figure 8(a,c)*).

Simulations of accommodative lag as a function of refractive error for the reciprocal condition are shown for the two models and their difference in *Figure 9(a),(b)*, and *(c)* respectively Similar trends occur as observed in *Figure 8*. As found with heterophoria, steady state errors of accommodation associated with a given refractive error remained fairly constant for various reciprocal combinations of cross-link ratios. Comparison of the simulations of the adaptive and non-adaptive models illustrates that tonic adaptation reduced the steady state errors of

accommodation over the entire range of myopia with the largest reductions for low values of the CA/C ratio combined with high values of the AC/A ratio (*Figure 9(a,c)*).

Discussion

Interactions between biases (refractive error and heterophoria) and cross-link gains

Simulations of both models indicate that both uncorrected hyperopia and esophoria increase the lag of accommodative and uncorrected myopia and exophoria decrease the lag or introduce a lead of accommodation in response to the near (40 cm) stimulus. These effects were increased when gain of either cross-
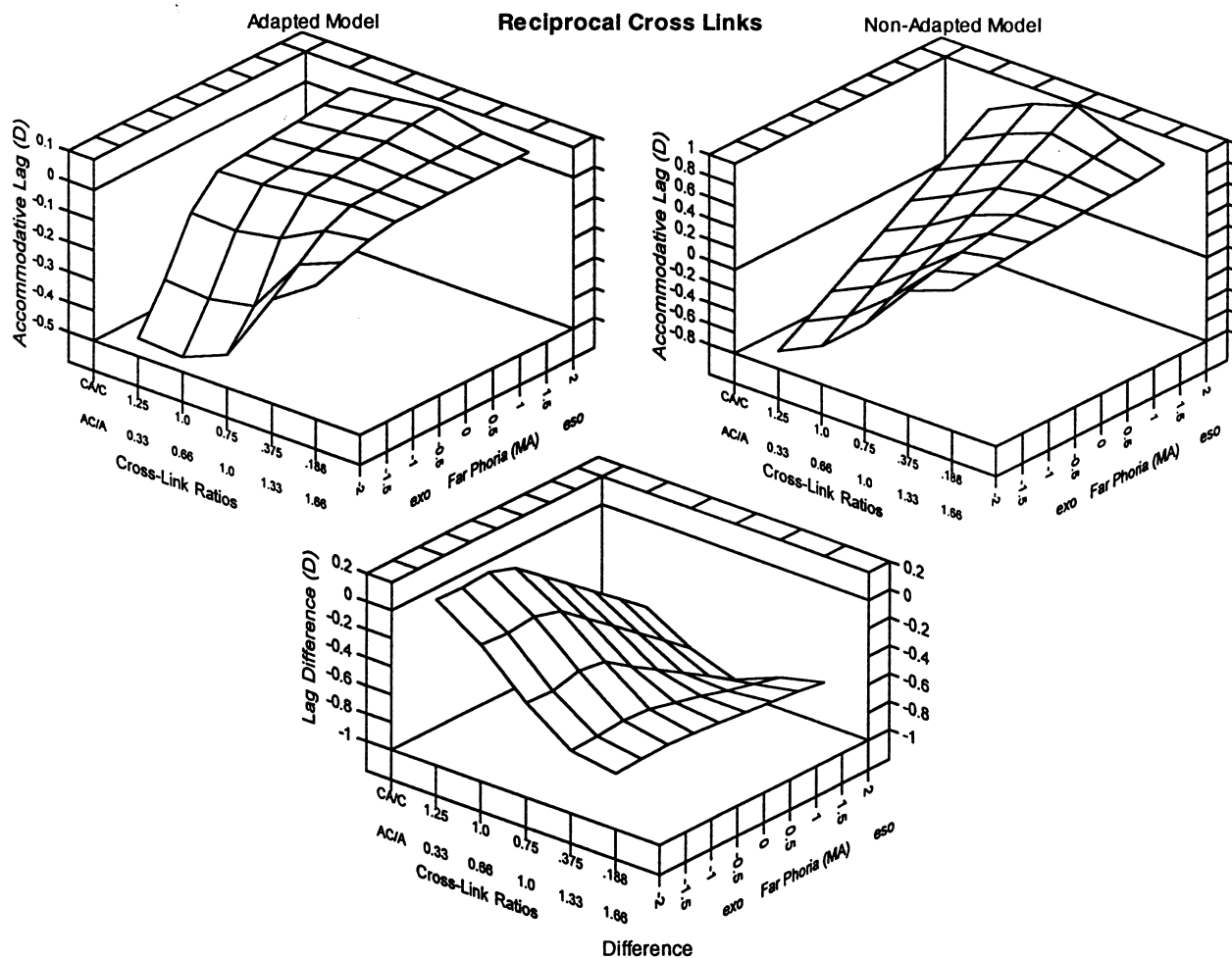
Figure 8. Simulations of accommodative lag as a function of distance heterophoria for the reciprocal condition are shown for the adaptable and non-adaptable models and their difference in (a), (b), and (c) respectively. (a) and (b) illustrate that the steady state error of accommodation (leads) increased with exo values of heterophoria and the steady state errors remained constant over the range of reciprocally combined AC/A and CA/C ratios; (c) plots the difference between predictions of the adaptable (a) and the non-adaptable (b) model and illustrates that adaptation reduced the steady state errors of accommodation over the entire range of heterophoria with the largest reductions for low values of the CA/C ratio combined with high values of the AC/A ratio.

link, accommodative convergence (AC/A) or convergence accommodation (CA/C), was increased within a moderate range of values while the other was fixed at a normal value (clamped condition). Under the clamped CA/C conditions, abnormally high accommodative convergence caused the accommodative response to lag when the far phoria and refractive error were zero because of the large near esophoria produced by the high AC/A ratio. Similarly, under clamped AC/A conditions, abnormally high convergence accommodation caused the accommodative response to lead its stimulus when the far phoria and refractive error were zero because of the large amount of convergence accommodation stimulated by the high CA/C ratio. These errors of accommodation produced

by biases of vergence and accommodation were exaggerated when both the AC/A and CA/C ratios were increased (covaried condition) and affects of cross-link gain were negated when an increase of one cross-link (e.g. AC/A) was accompanied by a reduction of the other cross-link (e.g. CA/C) (reciprocal condition).

Larger steady state errors of accommodation were produced in the clamped conditions by changes in the AC/A than the CA/C ratio. This can be seen by comparing the slopes of the simulations along the X axis in *Figure 2* and *3* compared to *Figure 4* and *5*. The slopes are steeper in the former graphs in which the AC/A was varied while the CA/C was clamped. This is related to the greater range of AC/A than CA/C values and to the lower values of the clamped AC/A
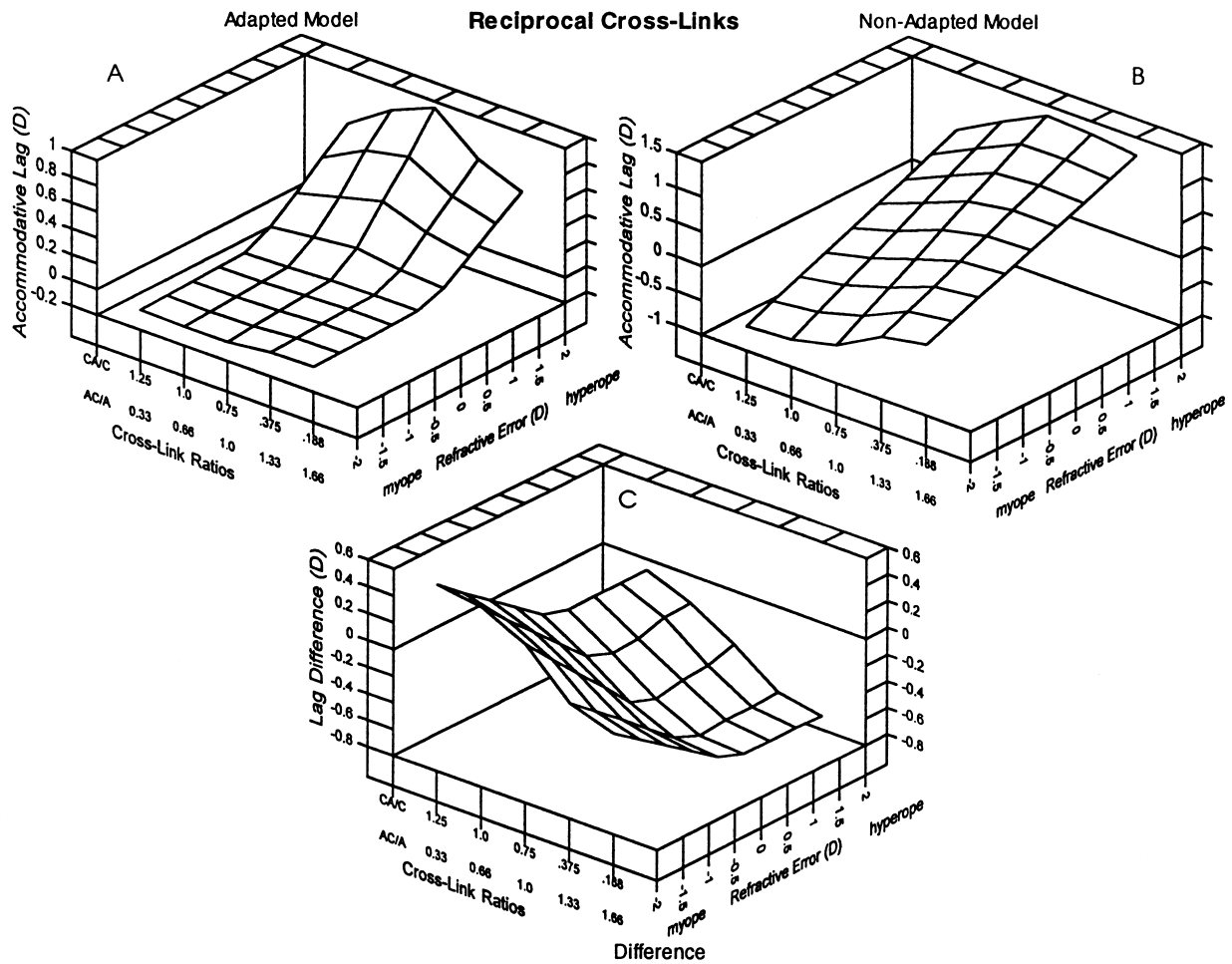
Figure 9. Simulations of accommodative lag as a function of refractive error for the reciprocal condition are shown for the adaptable and non-adaptable models and their difference in (a), (b), and (c) respectively. (a) and (b) illustrate that the steady state error of accommodation (lags) increased with hyperopic values of refractive error and the steady state errors remained constant over the range of reciprocally combined AC/A and CA/C ratios. (c) plots the difference between predictions of the adaptable (a) and the non-adaptable (b) model and illustrates that adaptation reduced the steady state errors of accommodation over the entire range of refractive errors with the largest reductions for low values of the CA/C ratio combined with high values of the AC/A ratio.

(0.66) than the clamped CA/C (0.75). These clamped values were chosen because they represent population norms. However, if the clamped values for the two cross links had both been 1.0, the affects of AC/A and CA/C variations would have been more alike.

Effects of adaptation on lag of accommodation

The inclusion of tonic adaptation in the model reduced steady state errors of accommodation for all conditions except when the AC/A ratio was very high (e.g. 2 MA/D or 12Δ/D). Tonic adapters of accommodation and convergence serve two functions. One is to relieve the activity of the phasic system which results in a reduction of steady state errors or lag of accommodation (Schor, 1979b; 1980; Hung and Semmlow,

1980). The other function is to enhance the gain of the cross-links between the two systems (Schor and Kotulak, 1986a). The phasic controller of accommodation is the main stimulus to accommodative vergence (Schor and Kotulak, 1986a). When tonic accommodation takes over the control of accommodation there is a reduction in the phasic stimulus to accommodative vergence. However accommodative vergence is maintained by adaptable tonic vergence which stores the accommodative vergence input and in this way it enhances the cross-link interaction. In the current model, each cross link is stimulated by phasic but not tonic activity in the originating system and the cross-link is facilitated by feeding into the tonic controller of the receiving system. This tonic enhancement of cross-link input is compatible with stable steady-

state interactions for normal cross-link gains (Schor, 1979b) but it causes instability when the gains are abnormally large. Under these conditions, the resulting large cross-link interactions (e.g. excessive convergence accommodation) cause excessive stimulation of the phasic accommodative controller and larger steady state errors result compared to models in which there are no tonic controllers.

The tonic adapters serve the same two functions in models that place cross links at the end of the feed-forward loop (Ebenholtz and Fisher, 1982; Rosenfield and Gilmartin, 1988; Hung, 1992) rather than between the phasic and tonic elements (Schor and Kotulak, 1986a). For normal cross-link values, the tonic controllers reduce the burden on the phasic controller and its associated steady state error. This organization also augments the mutual interactions between the two systems. Cross-links are stimulated in the originating loop by the sum of phasic and tonic controllers. As with the other model, when the cross-link gain is high, enhancement by the input from the tonic controller results in excessive convergence accommodation. These conditions place additional demands on the phasic accommodative controller and result in a larger steady state error than if there had been no adaptable tonic controllers. Indeed, simulations not shown here demonstrate the same pattern of steady state errors in adaptable models that place cross-links shown in *Figure 1* at a point in the feed forward loop after the phasic and adaptable tonic controllers (Ebenholtz and Fisher, 1982; Rosenfield and Gilmartin, 1988; Hung, 1992). The large lags predicted for high cross-link gains at either location (before or after tonic elements) combined with hyperopia would challenge the fusional vergence limits of normal binocular vision and are often associated with accommodative esotropia (Von Noorden, 1996). In most non-strabismic cases where the AC/A does not assume these extreme values, enhanced tonic accommodation and tonic vergence could potentially reduce the progression of myopia by reducing blur produced by steady state errors of accommodation.

Combined parameter effects on accommodative lag

The simulations of the models shown in *Figure 1* demonstrate that the lag of accommodation depends upon a combination of factors and can not be predicted on the basis of isolated factors such as AC/A ratio, heterophoria or refractive error. A high AC/A ratio can be associated with a large lag of accommodation if accompanied by a normal or high CA/C ratio and either hyperopia or esophoria. The same high AC/A ratio can be associated with a normal or even low lag of accommodation if accompanied by a

low CA/C ratio, especially in association with either exophoria or myopia. Adaptation of accommodation and vergence minimize the lag in the presence of heterophoria or refractive error as long as the AC/A is not extremely large or in the range that is normally associated with accommodative esotropia.

Covaried and reciprocal patterns of cross-link interactions

Combinations of cross-link interactions between accommodation and convergence that resemble either clamped or reciprocal patterns occur naturally in clinical populations (Schor and Horner, 1989). The reciprocal pattern of cross-links in which the AC/A ratio is high and the CA/C ratio is low is associated with low adaptability of accommodation and high adaptability of vergence. Similarly, when the CA/C ratio is high and the AC/A ratio is low this reciprocal pattern of cross-links is associated with high adaptation of accommodation and low adaptation of vergence. When the adaptability of vergence and accommodation is balanced by fatiguing the stronger tonic element, the AC/A and CA/C ratios change to normal values (Schor and Tsuetaki, 1987). The current paper suggests that this reciprocal pattern of cross-links will minimize steady state errors of accommodation associated with uncorrected refractive error or heterophoria. In contrast, cross-link patterns of a high AC/A ratio associated with a normal or high CA/C ratio or visa versa could exacerbate steady state errors of accommodation associated with refractive errors or heterophoria. If the steady state errors of accommodation influence the emmetropization process, then these two patterns of cross-link interactions could affect the progression of myopia differently.

Implications for emmetropization

The role that the lag of accommodation might play in the emmetropization process is speculative (Flitcroft and Eustace, 1997; Gwiazda *et al.*, 1995; Goss and Wickham, 1995; Goss, 1985). Comparative studies indicate that changes in axial length occur in response to the sign of retinal image blur (Schaeffel *et al.*, 1988; Irving *et al.*, 1991; Wildsoet and Wallman, 1995; Hung *et al.*, 1995). If the sign of myopic and hyperopic steady state errors of accommodation can be distinguished, and if the focus errors are large enough to stimulate the emmetropization process, lags of accommodation could exacerbate the progression of myopia while leads of accommodation might reduce it.

Two risk factors associated with myopia that would increase steady state errors of accommodation are a high AC/A ratio and esophoria (Jiang, 1995; Goss and

Zhai, 1994). The impact of the elevated AC/A on the lag of accommodation is diminished in young myopes by a concurrent reduction of the CA/C ratio (Bobier *et al*., 1998). The combined elevated AC/A and reduced CA/C could result from either a reduction of adaptable tonic accommodation or an increase of adaptable tonic vergence (Schor and Tsuetaki, 1987). An increase in adaptable tonic accommodation could potentially reduce the progression of myopia in two ways. First, it would reduce the amplitude of the lag of accommodation (Schor and Kotulak, 1986b; Rosenfield and Gilmartin, 1998), and second it would reduce the AC/A ratio by lowering the amount of phasic stimulation of accommodative vergence (Schor and Kotulak, 1986a). Models of accommodation predict that the combined increase of the AC/A with esophoria would tend to increase the lag of accommodation when associated with hyperopia, and decrease the lag or produce a lead when associated with myopia. Thus the accommodative lag should be small or absent in myopia. However, myopes still exhibit lags rather than leads of accommodation (McBrien and Millodot, 1986; Gwiazda *et al*., 1995), particularly while the myopia is still progressing (Abbott *et al*., 1998). It should be noted that these accommodative response functions were measured under monocular viewing conditions with full correction of refractive error. The same individuals who show lags of accommodation under these conditions might exhibit leads of accommodation under normal binocular conditions without refractive corrections. The lag of accommodation measured under laboratory conditions could result from a strategy used to reduce a lead of accommodation under normal uncorrected binocular viewing conditions. Thus other factors than accommodative lag could influence the progression of uncorrected myopia. In the case of fully corrected myopes, progression of refractive error could be related to the lag of accommodation that is influenced by vergence bias, i.e. heterophoria, and accommodative bias, i.e. the resting focus of accommodation.

Acknowledgements

References

Abbott, M. L., Schmid, K. L. and Strang, N. C. (1998). Differences in the accommodation stimulus response curves of adult myopes and emmetropes. *Ophthalmic and Physiological Optics* **18**, 13–20.

Alpern, M. and Ellen, P. (1956). A quantitative analysis of the horizontal movements of the eyes in the experiments of Johannes Muller. I Methods and results. *Am. J. Ophthalmol.* **42**, 289–303.

Bobier, W. R., Epp, K. L. and Stephen, C. M. (1998). Convergence-accommodation is reduced in young myopes. *Invest. Ophthalmol & Vis. Sci.* **39**(4) ARVO Suppl abs 2981. p. S640. .

Ebenholtz, S. M. and Fisher, K. (1982). Distance adaptation depends upon plasticity in the oculomotor control system. *Perception & Psychophysics* **31**, 551–560.

Fincham, E. F. (1955). The proportion of ciliary muscular force required for accommodation. *J. Physiol. Lond.* **128**, 99–112.

Fincham, E. F. and Walton, J. (1957). The reciprocal actions of accommodation and vergence. *J. Physiol. Lond.* **137**, 488–508.

Flitcroft, D. I. and Eustace, P. (1997). Emmetropization and late onset myopia: the role of retinal image quality and the accommodation system. *Invest. Ophthalmol & Vis. Sci.* **38**, ARVO abstract 2156. p. S461. .

Flom, M. C. (1960). On the relationship between accommodation and accommodative convergence. II Stability. *Am. J. Optom. Arch. Am. Acad. Optom.* **37**, 517–23.

Goss, D. A. 1988. Retinal image-mediated ocular growth as a possible aetiological factor in juvenile-onset myopia. Vision Science Symposium/A tribute to Gordon Heath. Indiana University, Bloomington. pp. 165–183. .

Goss, D. A. and Wickham, M. G. (1995). Retinal-image mediated ocular growth as a mechanism for juvenile onset myopia and for emmetropization. A literature review. *Doc. Ophthalmol.* **90**, 341–375.

Goss, D. A. and Zhai, H. (1994). Clinical and laboratory investigations of the relationship of accommodation and convergence function with refractive error. A literature review. *Doc. Ophthalmol.* **86**, 349–380.

Green, D. G., Powers, M. K. and Banks, M. S. (1980). Depth of focus, eye size and visual acuity. *Vision Research* **20**, 827–835.

Gwiazda, J., Bauer, J., Thorn, F. and Held, R. (1995). Shifts in tonic accommodation after near work are related to refractive errors in children. *Ophthalmic and Physiological Optics* **15**, 93–97.

Gwiazda, J., Thorn, F., Bauer, J. and Held, R. (1993). Myopic children show insufficient accommodative response to blur. *Invest. Ophthalmol Vis. Sci.* **34**, 690–694.

Hoffmann, F. B. and Bielchowsky, A. (1900). Uber die der Wilkue entzogenen Fusions-Bewegungen der Augen. *Arch. Gesample Physiol.* **80**, 1–40.

Hofstetter, H. W. 1983. Graphical Analysis. ed. C. M. Schor and K. Ciuffreda. In: *Vergence Eye Movements: Basic and Clinical Aspects*, Butterworths, Boston, pp. 439–464.

Hung, G. K. (1991). Linear model of accommodation and vergence can account for discrepancies between AC/A measures using the fixation disparity and phoria methods. *Ophthal. Physiol. Opt.* **11**, 275–278.

Hung, G. K. (1992). Adaptation model of accommodation and vergence. *Opthal. Physiol. Opt.* **12**, 319–326.

Hung, L. F., Crawford, M. L. J. and Smith, E. L. (1995). Spectacle lenses alter eye growth and the refractive status of young monkeys. *Nature Med.* **1**, 761–765.

Hung, G. K. and Semmlow, J. L. (1980). Static behavior of accommodation and vergence: computer simulation of an interactive dual-feedback system. *IEEE Trans. Biomed. Eng.* **27**, 439–447.

Irving, E. L., Callender, M. G. and Sivak, J. G. (1991). Inducing myopia, hyperopia, and astigmatism in chicks. *Optom. Vis. Sci.* **68**, 364–368.

Jiang, B. (1995). Parameters of accommodative and vergence systems and the development of late-onset myopia. *Invest. Ophthalmol. Vis. Sci.* **36**, 1737–1742.

Jiang, B. C. (1996a). Dark focus and dark vergence: an experimental verification of the configuration of the dual-interactive feedback model. *Ophthal. Physiol. Opt.* **16**, 342–347.

Jiang, B. C. (1996b). Accommodative vergence is driven by the phasic component of the accommodative controller. *Vision Res.* **36**, 97–101.

Judge, S. J. and Cumming, B. G. (1986). Neurons in the monkey midbrain with activity related to vergence eye movement and accommodation. *J. Neurophysiol.* **55**, 915–30.

Kotulak, J. and Schor, C. M. (1986a). The accommodative response to sub-threshold blur and to perceptual fading during the Troxler phenomenon. *Perception* **15**, 7–15.

Kotulak, J. and Schor, C. M. (1986b). The dissociability of accommodation from vergence in the dark. *Invest. Ophthal. & Vis. Sci.* **27**, 544–551.

Lakkis, G. and Bruce, A. S. (1989). The effect of vergence adaptation on convergent accommodation. *Ophthalmic and Physiol. Optics* **9**, 97–98.

Mays, L. E. and Gamlin, P. D. R. (1995a). Neuronal circuitry controlling the near response. *Curr. Opin. Neurobiol.* **5**, 763–8.

McBrien, N. A. and Millodot, M. (1986). The effect of refractive error on the accommodation response gradient. *Ophthalmic and Physiological Optics* **6**, 145–149.

Ogle, K. N. (1966). The accommodative convergence accommodation ratio and its relation to the correction of refractive error. *Trans. Am. Acad. Ophthalmol. Otolaryngol.* **70**, 322–30.

Polak, N. A. and Jones, R. (1990). Dynamic interactions between accommodation and convergence. *IEEE Trans on Biomed Engineering* **37**, 1011–1014.

Riggs, L. A. and Neihle, W. (1960). Eye movements recorded during convergence and divergence. *J. Opt. Soc. Am.* **50**, 913–920.

Rosenfield, M. and Gilmartin, B. (1988). Accommodative adaptation induced by sustained disparity-vergence. *Am. J. Optom. Physiol. Opt.* **65**, 118–12615.

Rosenfield, M. and Gilmartin, B. (1998). Accommodative adaptation during sustained near vision reduces accommodative error. *Invest. Ophthalmol. & Vis. Sci.* **39**(4) ARVO Suppl abs 2979. p. S639. .

Schaeffel, F., Glasser, A. and Howland, H. C. (1988). Accommodation, refractive error and eye growth in chickens. *Vision Research* **28**, 639–657.

Schor, C. M. (1979a). The influence of rapid prism adaptation upon fixation disparity. *Vision Research* **19**, 757–765.

Schor, C. M. (1979b). The relationship between fusional vergence eye movements and fixation disparity. *Vision Research* **19**, 1359–1367.

Schor, C. M. (1980). Fixation disparity: steady-state error of disparity induced vergence. *Am. J. Optom.* **57** (9), 618–631.

Schor, C. M. (1988). Imbalanced adaptation of accommodation and vergence produces opposite extremes of the AC/A and CA/C ratios. *Am. J. Optom. & Physiol. Optics* **65** (5), 341–348.

Schor, C. M. (1992). A Dynamic Model of Cross-Coupling Between Accommodation and Convergence: Simulation of Step and Frequency Responses. *Optom. and Vis. Sci.* **69**, 258–269.

Schor, C. M. and Horner, D. (1989). Adaptive disorders of accommodation and vergence in binocular dysfunction. *Ophthalmic and Physiol Opt.* **9**, 264–268.

Schor, C. M., Johnson, C. and Post, R. (1984). Adaptation of tonic accommodation. *Ophthalmic and Physiol. Optics* **4** (2), 133–137.

Schor, C. M. and Kotulak, J. (1986a). Dynamic interactions between accommodation and convergence are velocity sensitive. *Vision Res.* **26**, 927–942.

Schor, C. M. and Kotulak, J. (1986b). Adaptation of tonic accommodation reduces accommodative lag and is masked in darkness. *Invest. Ophthal.* **27**, 820–827.

Schor, C. M. and McLin, L. N. Jr (1988). The effect of luminance on accommodative and convergence aftereffects. *Clin. Vis. Sci.* **3** (2), 143–154.

Schor, C. M. and Narayan, V. (1982). Graphical analysis of prism adaptation, convergence accommodation and accommodative convergence. *Am. J. Optom. and Physiol. Optics* **59** (10), 774–784.

Schor, C. M. and Tsuetaki, T. (1987). Fatigue of accommodation and vergence modifies their mutual interactions. *Invest. Ophthalmol. & Vis. Sci.* **28**, 1250–1259.

Sheedy, J. and Saladin, J. 1983. Validity of diagnostic criteria and case analysis in binocular vision disorders. ed. C. M. Schor and K. Ciuffreda. In: *Vergence Eye Movements: Basic and Clinical Aspects*, Butterworths, Boston, pp. 517–540.

Tsuetaki, T. and Schor, C. M. (1987). Clinical method for measuring adaptaiton of tonic accommodation and vergence accommodation. *Am. J. Optometry and Physiol. Optics* **64**, 437–449.

Von Noorden, G. K. 1996. Binocular vision and ocular motility: theory and management of strabismus. 5th edn. St. Louis: Mosby. .

Wallman, J. and McFadden, S. (1995). Monkey eyes grow into focus. *Nature Medicine* **1**, 737–739.

Wick, B. and London, R. (1987). Analysis of binocular visual functions using tests made under binocular conditions. *Am. J. Optom. Physiol Opt.* **64**, 227–240.

Wildsoet, C. and Wallman, J. (1995). Choroidal and scleral mechanisms for compensation for spectacle lenses in chicks. *Vision Research* **35**, 1175–1194.